Experimental study of mitigation systems to prevent Thermal Runaway of Li-ion Batteries

Experimental study of mitigation systems to prevent Thermal Runaway of Li-ion Batteries

Francesco D'Annibale, Carla Menale

ENEA – Italian National Agency for New Technologies, Energy and Sustainable Economic Development, Casaccia Research Center, Via Anguillarese, 301 – 00123 S. Maria di Galeria (RM), Italy

carla.menale@enea.it

Abstract. Li-ion batteries have experienced a widespread deployment due to the strong interest in electrochemical devices capable of storing a large amount of energy in small volumes and supplying high powers when required. However, besides those advantages, this technology still presents several unsolved issues, especially regarding the safety aspects. These devices can, in fact, experience thermal runaway if the generated thermal power is not adequately dispersed, and this can occur when the cell / battery is subjected to abuse conditions (mechanical, electrical or thermal abuses).
The experimental study was carried out using a full-scale hardware simulator, capable of simulating the thermal behavior of a battery pack, where electrically heated elements replaced real Li-ion cells. This expedient guarantees a high reproducibility of the working conditions and consequently a higher reliability of the measured data.
The hardware simulator allows to reproduce the thermal behavior under normal operating conditions, and under abuse conditions which can lead to thermal runaway.
The present work reports the results of the tests that have been carried out by reproducing the abuse conditions in one cell inside a battery module; the abused cell is heated with a high power (from 100 to 500 W for cells with a maximum heat loss of 30 W under normal operating conditions) and the efficiency of different cooling systems is checked both in limiting the temperature of the abused cell and in preventing the propagation of heat to the adjacent cells. In particular, different fluids, different fluid speeds and different mitigation methods have been tested.

1. Introduction

Due to the advantages of high power, high cycling life and large specific energy, Li-ion batteries (LIBs) are currently used in most portable consumer electronics such as cell phones, laptop computers and they are also the main energy storage element of electric vehicles (EVs), and stationary electrochemical energy storage systems (ESSs). However, the battery performance is greatly affected by the operating temperature. Both the high temperature of batteries and the poor uniformity of battery modules could affect the electrochemical reactions, durability, life cycle and safety [1, 2].
Furthermore, Li-ion battery cell temperature over 80 °C can possibly initiate its thermal runaway [3].
Consequently, thermal management is always a hot topic for lithium ion batteries: a highly efficient battery thermal management system (BTMS) is needed to guarantee the batteries to operate in the optimal condition.

Numerous experimental and numerical studies have been conducted on the active and passive cooling methods of the battery system [4-6].

The air and liquid cooling are conventional methods which have been widely adopted in commercial electrical vehicles and stationary energy storage systems. The merits of active air cooling include the low cost, simplicity and easy availability of coolant materials.

The mutual problem of the forced air and liquid thermal management is that the addition of extra components such as valves, blowers/pumps and cooling ducts/channels will raise the weight and space utilization of BTMSs. For this reason, passive thermal management techniques that take advantages of latent heat during the phase change process can be employed. In a particular way, the battery TMSs being based on PCMs have been widely studied in the last years and the role of various additives like metal foams, has been the focal point of an array of research studies [7,8].

Recently, also passive BTMSs using the latent heat of liquid-vapor phase change process, including heat pipes, have been studied [9,10].

Anyway, experimental tests with li-ion batteries under abuse conditions are hardly feasible. Most of the experimental studies relating to thermal management systems for battery packs are carried out under normal operating conditions and not under abuse conditions due to safety problems [11, 12].

In addition, in the current literature, little attention has been paid to dielectric coolants in direct contact with batteries. However, a key safety advantage that Single-Phase Dielectric Coolants (SLICs) is that they can be brought into direct contact with all components of the system without causing shorting failures of electronics or shock hazard to users.

In order to test the efficiency of different cooling systems in limiting the temperature of an abused cell in a battery module and in preventing the propagation of heat to the adjacent cells, an experimental facility has been setup. The batteries have been replaced with electrically heated elements characterized by the same thermal behavior of the real cells: the adoption of a simulation facility instead of real cells guaranteed a high reproducibility of the working conditions. Furthermore, abuse conditions can be reproduced avoiding the safety issues for people and facilities.

2. Experimental setup

2.1. Battery hardware simulator

An hardware emulator [1] has been set up to reproduce the thermal behavior of a battery pack, where electrically heated elements replaced real Li-ion cells.

This expedient has a number of advantages with respect to the use of real cells: there are no changes of the resistance and the performance of the cells over time due to the aging effects; the simulator also allows working under “extreme” operating conditions representative of thermal abuse of the cells with no risk; there is no need to recharge the battery after each test, so experimental tests can be performed much faster; only the heat generated in the battery must be supplied, which is about 1/10 of the energy required for charging.

The experimental system has been setup referring to commercial EIG-C020 pouch cells (Capacity = 20Ah, Rint = 3 mΩ): a pack of four pouch cells has been simulated by four electric heaters (

Figure 1) contained in four composite (metal and plastic) boxes with the same characteristics of the real cells, in terms of geometrical configuration, thermal capacity and resistance. The main properties of the test cells are compared with those of commercial EIG-C020 pouch cells in Table 1.

One of the four cells was also provided with an additional resistance (Figure 3a), located close to the electrodes, which could be occasionally activated to simulate the generation of hot spots already detected on real aged cells [1]. In addition, a “Thermal Runaway” cell was made (Figure 3b): this cell could be subjected to a larger heat input, and could replace one of the former cells in the test pack, to assess the efficiency of the cooling system under typical conditions which could lead to a thermal runaway. The maximum power provided to the adopted resistances were: 60 W for the “standard” cell, 27 W for the localized resistance and 500 W for the “thermal runaway” cell.

All cells have been preliminarily tested under different transient conditions, and the temperature distribution of each face of the 4 cells have thus been mapped using an IR camera (FLIR S60): the results showed that all the cells behave in the same way, with almost identical average and maximum temperatures on all cells [1].

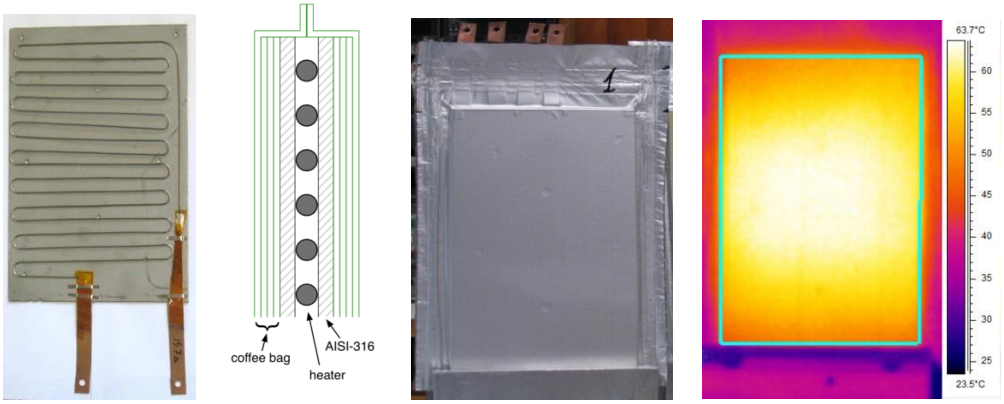

(a) (b) (c)

Figure 1. a) thermal resistances; b) test cell; c) thermal image

Table 1. Main characteristics of a real EIG-C020 cell and of a test cell

	EiG-C020 cell	*Test cell*
L [m] x H [m]	0.125x0.194	0.125x0.194
s [m]	7.00E-03	4.80E-03
k [W/m K]	0.72	0.731
Rt [K/W]	0.00243	0.00260
M*cp [J/K]	341.5	339.3

2.2. Experimental rigs for cooling tests

Two separate facilities have been set up to test different cooling fluids, under various working conditions.

The main components of the liquid cooling loop were (Figure 2a): a volumetric gear pump, a Coriolis flow-meter, a pre-heater and a compact heat exchanger to cool down the fluid before pump inlet. The cells were vertically oriented and contained in a box (immersion cooling test) provided with one thermocouple at the entrance to measure the inlet temperature and two thermocouples after the battery pack to measure the outlet temperature of the cooling fluid. The pre-heater and the volumetric pump could be adjusted to maintain the values of the inlet temperature and the mass flow rate at the set points. The tested cooling fluids were a silicone-oil (Clearco-50cSt) and a perfluorinated polyether (Galden HT135): these fluids were selected because they are heat transfer fluids engineered for high temperature applications with different characteristics from each other. The properties are shown in Table 2.

Table 2. Dielectric fluid properties

	Cp (J/kg K)	*k (W/m K)*	*ρ (kg/m^3)*	*μ (kg/m s)*	*Type*
Galden HT135	962.68	0,065	1720	$1.72 \cdot 10^{-3}$	Perfluorinated polyether
Clearco-50 cSt	1500	0,15	960	$4.8 \cdot 10^{-2}$	Silicone oil
Air	1004.1	0,026	1.17	$1.83 \cdot 10^{-5}$	Air

The main components of the air cooling loop (Figure 2b) were: four axial fans; an electric pre-heater to control the air inlet temperature; an anemometer; a channel, long enough to allow a fully developed velocity profile and a proper operation of the anemometer; the test section with a thermocouple (to measure the inlet air temperature) and the battery module (the same four cells of previous case); an air mixing device and two thermocouples to measure the outlet air temperature.

The cells in the module were monitored by 14 calibrated thermocouples (type k, accuracy of ±0.1°C) to measure their surface temperature.

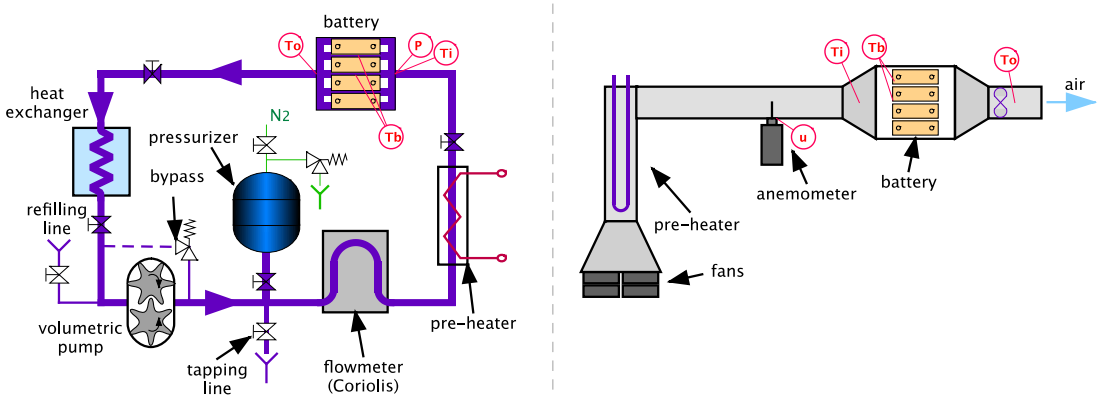

(a) (b)

Figure 2. Schematic diagrams of the cooling loops: a) for liquids, b) for air.

3. Results and discussion

Tests to simulate abuse conditions were performed by providing high power to the Thermal Runaway (TR) cell, while the other cells have been provided with a power of 30 W or 0 W to verify the effect of an excessive heating of the TR cell on the other cells in the module.

The power provided to the TR cell (W_{TR}) was: 100, 300 or 500 W. For each tested fluids three graphs have been reported for a provided power of: 1) 300 W to the TR cell, 2) 300W to the TR cell and 30 W to the other cells (W_{norm}) and finally 3) 500 W to the TR cell. The temperature of the TR cell and the temperature of the opposite face of one of the two adjacent "normal" cells are shown in the graphs.

In this way, it is possible to simulate three types of pre-incidental events: 1) the beginning of the Thermal Runaway phenomenon in a cell with the subsequent intervention of the Battery Management System (BMS) to detach the other cells, 2) the beginning of the Thermal Runaway phenomenon in a cell with no intervention of the BMS: the other cells continue to feed the utilities; finally 3) the same condition of the point 1, but with a greater thermal power provided to the TR cell to evaluate the effect of its variations. For this purpose, few tests were also performed providing a lower power to the TR cell.

The effect of the power increase on the temperature of the TR cell, is remarkable using air as cooling fluid. Increasing the provided power from 300 W (Figure 3 and Figure 4) to 500 W (Figure 5), for the same air velocity, after 3 minutes the temperature of the TR cell increase of 60°C more (it is equal to 120°C with a provided power of 300 W and exceeds 180°C with a provided power of 500 W)

The heating of the other cells in the module has no effect on the temperature of the TR cell and it is quite small on the other cells. However, the cells close to the TR cell are warmed up by it, especially with low air speeds. For example with an air velocity of 0 m/s with a provided power of 300 W to the TR cell, the adjacent cells can exceed 40°C after 3 minutes if they don't have internal heat generation, but the cells can exceed 54°C if they are powered with 30 W; using an air velocity of 2 m/s the temperature varies from 31 to 41°C, respectively without and with heat generation.

In addition, air cooling has proved unsuitable for batteries working under abuse conditions, as the cell involved would exceed 90°C in a fairly fast time (around a minute) even with a very high air speed: the first section of the climb is almost independent from the air velocity in all three graphs (Figure 3, Figure 4 and Figure 5).

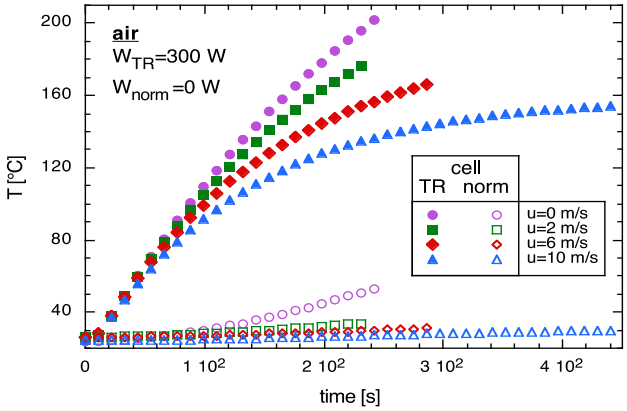

Figure 3. Air at different fluid velocities: TR cell and "normal"cell - W_{TR}=300 W, W_{norm}=0W

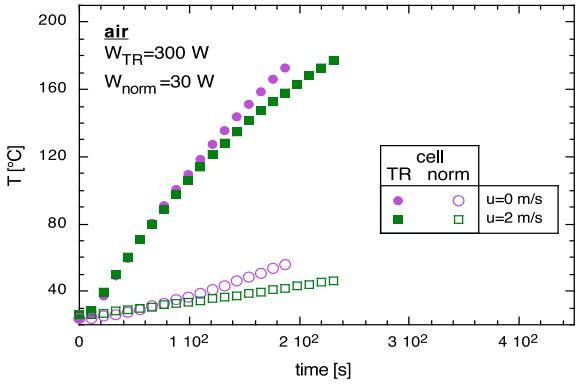

Figure 4. Air at different fluid velocities: TR cell and "normal"cell - W_{TR}=300W, W_{norm}=30W

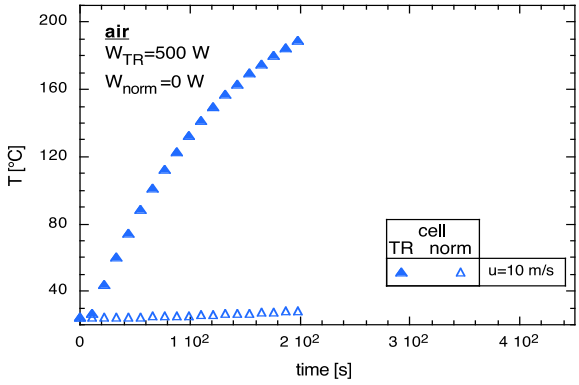

Figure 5. Air at different fluid velocities: TR cell and "normal"cell - W_{TR}=500W, W_{norm}=0W

Using the Galden-HT135 (see Table 2) liquid, the results are completely different, allowing, even when the liquid is still, to contain the temperature of the hot cell below 80°C when W_{TR}=300 W (Figure 6 and Figure 7) and just above 80°C when W_{TR}=500W (Figure 8). The adjacent cells are heated by the liquid layer at temperatures even higher than that obtained using air. This happens because with liquids the heating triggers a natural convection that is added to the forced one and, since very low liquid speeds have been used, the natural convection quickly becomes predominant.

This is the reason why the behaviour of the cells is almost the same, even when the liquid velocity is equal to 0 m/s and it is evidenced by the sharp change in slope between 60 and 100 s. It also explains the greater influence on adjacent cells: in its vertical motion in the 3 mm channel, the liquid at higher temperatures comes into contact with the other cell surfaces, heating them. The effect of the power increase from 300 to 500 W is practically zero, while the additional power of 30 W to the other cells generate a moderate increment of their temperature (with u=4 mm/s the temperature after 600 s is equal to 46°C when W_{TR}=300 W and 53°C when W_{TR}=500 W).

Using Galden it is possible to limit the consequences of the abnormal heating of a cell: it is possible to remove even 500 W avoiding an excessive temperature increase. It must also be kept in mind that

the pumping power with liquids is much lower: the order of magnitude goes from 10^{-6} to 10^{-4} W, while for air it goes from about 10^{-2} to 1 W. There is a ratio of 1/10000.

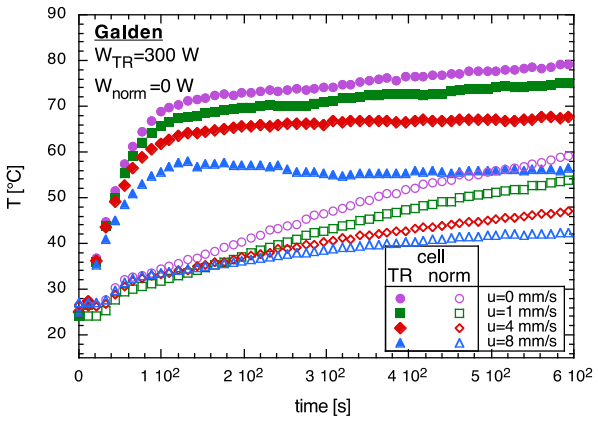

Figure 6. Galden at different fluid velocities: TR cell and "normal"cell - W_{TR}=300 W, W_{norm}=0W

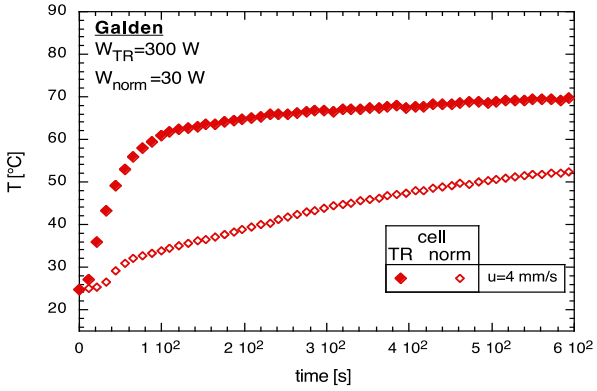

Figure 7. Galden at different fluid velocities: TR cell and "normal"cell - W_{TR}=300 W, W_{norm}=30W

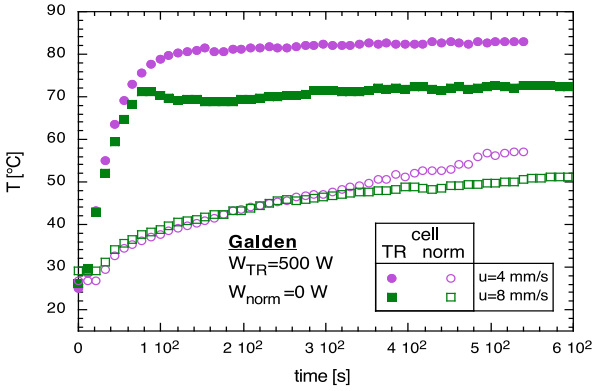

Figure 8. Galden at different fluid velocities: TR cell and "normal"cell - W_{TR}=500 W, W_{norm}=0W

The more viscous silicone oil Clearco PSF-50 shows worse results (Figure 9, Figure 10 and Figure 11) compared to the Galden liquid, although in some phases the behaviour is qualitatively similar. Also in this case, in fact, there is an overlap of the natural convection with the forced one, but it is much less evident (the change of slope is less noticeable and it takes place around 140 s for WTR=300 W).

Also in this case the temperature of the adjacent cells is influenced by the temperature increase of the TR cell, while the temperature increase of the other cells with the contribution of 30 W seems slightly less. The transition of the provided power to the TR cell from 300 W to 500 W has a noticeable influence on the temperatures, confirming that natural convection is less effective, mainly due to the increased viscosity (Table 2).

Another interesting comparison is that obtained with a lower power provided to the TR cell: W_{TR}=100 W, and W=30 W for the other cells in the module. In Figure 12 it is possible to see the temperature trend of the three cooling fluids for a typical fluid velocity. It is possible, also, clearly see the improvement in the passage from the air to Clearco and finally to Galden. Air and Clearco have a similar behavior in the first part, but after about 2 minutes the temperature of the TR cell stops rising

with Clearco while very high temperatures are reached with air. The temperature of the adjacent cells increases in the same way with air and Clearco, but much less with the Galden.

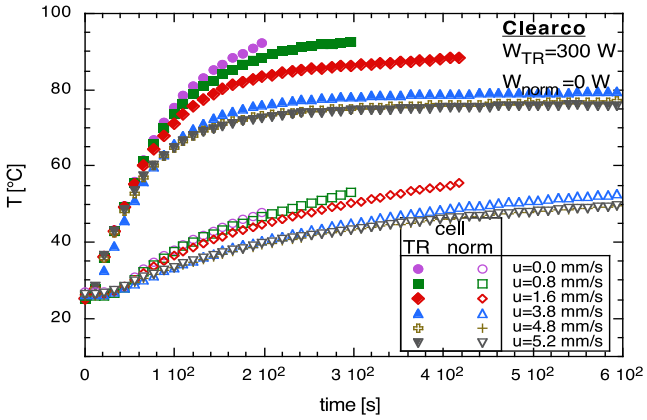

Figure 9. Clearco at different fluid velocities: TR cell and "normal"cell - W_{TR}=300 W, W_{norm}=0W

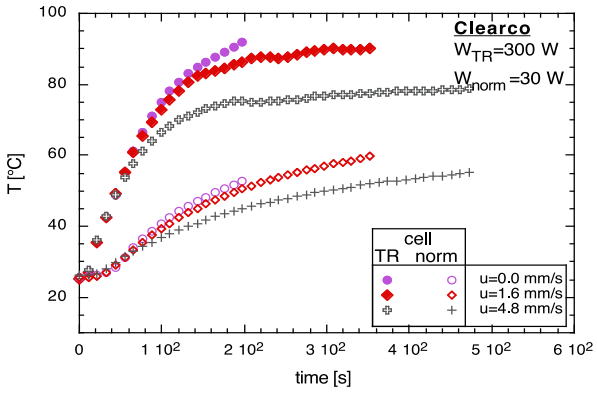

Figure 10. Clearco at different fluid velocities: TR cell and "normal" cell - W_{TR}=300W, W_{norm}=30W

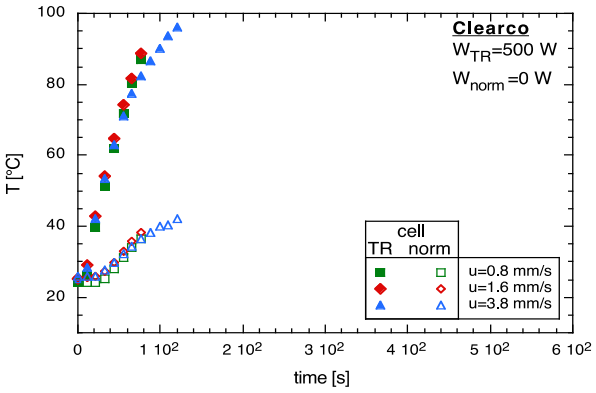

Figure 11. Clearco at different fluid velocities: TR cell and "normal" cell - W_{TR}=500 W, W_{norm}=0W

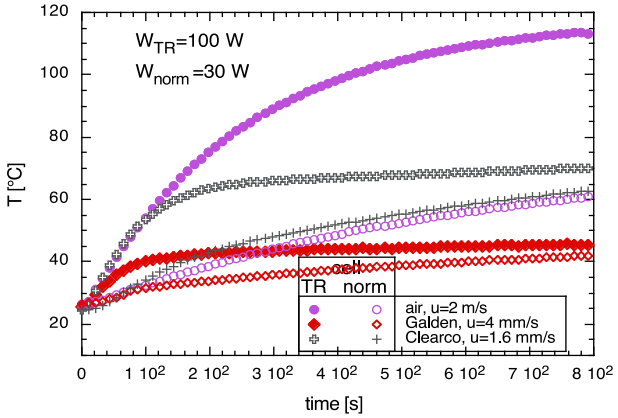

Figure 12. TR cell and "normal" cell – comparison between the three fluids: W_{TR}=100 W, W_{norm}=30 W

4. Conclusions

An experimental facility has been setup, capable of simulating the same behavior of real Li-ion pouch cells, which allowed assessing the efficiency of three cooling fluids in limiting the temperature of an abused cell. The adoption of a simulation facility instead of real cells guaranteed a high reproducibility of the working conditions and thus a higher reliability of the measured data. In addition, it allows working under "extreme" operating conditions representative of thermal abuse of the cells with no risk.

The tested cooling fluids were air and two liquids: a silicone-oil (Clearco-50cSt) and a perfluorinated polyether (Galden HT135). The battery cells are fully immersed in the dielectric heat transfer fluids (dielectric coolants). Liquid coolants have higher thermal conductivity and heat density than air, and therefore perform very effectively as a cooling medium. Air cooling has proved unsuitable for batteries working in abuse conditions, even using a high air velocity. On the contrary, using dielectric liquids as cooling fluids allows to limit the temperature rise: in a particular way the silicone oil manages to keep the temperature below 90 ° C only with high fluid velocities, while using Galden it is possible to work under safe conditions also using low liquid velocity.

Nomenclature

c_p = specific heat [J/kg K]
H = battery width [m]
k = thermal conductivity [W/m K]
L = battery height [m]
M = mass of the battery [kg]
R_t = thermal resistance of the battery = $\frac{s}{k}$ m^2 [K/W]
s = battery thickness [m]

Greek symbols
μ = viscosity [kg/m s]
ρ = density [kg/m^3]

References

[1] Menale C., D'Annibale F., Mazzarotta B., Bubbico R. 2019 *Energy* **182** 57-71.
[2] Feng X., Fang M., He X., Ouyang M., Lu L., Wang H., et al. 2014 *J. Power Sources* **255** 294-301.
[3] Ostanek J. K., Li W., Mukherjee P. P., Crompton K.R., Hacker C. 2020 *Applied Energy* **268** 114972.
[4] Zhao R., Zhang S., Liu J., Gu J. 2015 *J. Power Sources* **299** 557-567.
[5] Chen D., Jiang J., Kim G.H., Yang C., Pesaran A. 2016 *Appl. Therm. Eng.* **94** 846-854.
[6] Liu H., Wei Z., He W., Zhao J. 2017 *Energy Conversion and Management* **150** 304-330.
[7] Rao Z., Huo Y., Liu X., Zhang G. 2015 J. *Energy Inst.* **88** 241-246.
[8] Li W.Q., Qu Z.G., He Y.L., Tao Y.B. 2014 *J. Power Sources* **255** 9-15.
[9] Zhang Z., Wei K. 2020 *Applied Thermal Engineering* **166** 114660.
[10] Behi H., Karimi D., Behi M., Ghanbarpour M., Jaguemont J., Sokkeh M.A., Gandoman H.F., Berecibar M., Mierlo J.V 2020 *Applied Thermal Engineering* **174** 115280.
[11] Liu W., Jia Z., Luo Y., Xie W., Deng T. 2019 *Applied Thermal Engineering* **162** 114272.
[12] Pan M., Zhong Y. 2018 *International Journal of Heat and Mass Transfer* **126** 531-543.